

# Fourier Transform Infrared Spectroscopic Study of the Adsorption of CO and Nitriles on Na–Mordenite: Evidence of a New Interaction

Isabel Salla,<sup>\*,‡</sup> Tania Montanari,<sup>†</sup> Pilar Salagre,<sup>‡</sup> Yolanda Cesteros,<sup>‡</sup> and Guido Busca<sup>\*,†</sup>

*Dipartimento di Ingegneria Chimica e di Processo, Università di Genova, p.le J. F. Kennedy 1, I-16129 Genova, Italy, and Departament de Química Física i Inorgànica, Universitat Rovira i Virgili, pl. Imperial Tarraco, 1, 43005, Tarragona, Spain*

*Received: July 30, 2004; In Final Form: October 22, 2004*

The low temperature adsorption of CO and the room temperature adsorption of acetonitrile, propionitrile, isobutyronitrile, pivalonitrile, benzonitrile, and *o*-toluonitrile on Na–mordenite (NaMOR) have been investigated by Fourier transform infrared (FT-IR) spectroscopy. The results have been compared with analogous experiments performed on H–mordenite, Na–X zeolite, and Na–silica–alumina. The Na distribution in NaMOR has also been investigated by X-ray diffraction and far-IR spectroscopy. The conclusions are that Na<sup>+</sup> ion distribution is essentially random and that, together with the well-known interaction of the probes with Na<sup>+</sup> ions in the side pockets and the main channels, a stronger additional interaction occurs in all cases. This new interaction is likely multiple, involving either more Na<sup>+</sup> ions or Na and oxygen species. This interaction is more pronounced with the hindered nitriles, whose access at the main channels is likely forbidden. This suggests that this interaction, which is also observed on Na–X zeolites but not with Na–silica–alumina, occurs at the external mouths of the mordenite channels.

## Introduction

Zeolites in their protonic forms are largely used as environmentally friendly catalysts for proton-catalyzed reactions.<sup>1</sup> In particular, H–mordenite (HMOR) finds application for catalyzing efficiently the skeletal isomerizations of light alkanes such as butane and pentane.<sup>2</sup> Partially Na exchanged MOR (Na–HMOR) has been studied for application in xylene isomerization.<sup>3</sup> However, usually light alkali metal exchanged zeolites (e.g., NaX and NaY) act as quite mild basic catalysts,<sup>4–6</sup> whereas heavy alkali metal zeolites (such as CsY) are reported to be strong bases. In parallel, Na–zeolites show a mild Lewis acid behavior associated with the activity of highly unsaturated alkali metal cations that can adsorb electron-rich molecules, so allowing their separation.<sup>7</sup> Several studies have been reported recently concerning Na–mordenites. In particular, the effect of localization of Na<sup>+</sup> cations and of hydration have been studied by dielectric relaxation spectroscopy,<sup>8</sup> by thermally stimulated current measurement,<sup>9</sup> and by modeling.<sup>10</sup> The adsorption isotherms of small molecules such as N<sub>2</sub>, H<sub>2</sub>, and O<sub>2</sub> have been studied on Na–mordenite<sup>11,12</sup> and modified Na–mordenites.<sup>13</sup>

The low temperature adsorption of CO is today perhaps the most popular technique for characterizing adsorption sites of zeolites by IR spectroscopy. It actually allows a very detailed analysis of the surface sites as they appear at low temperature without strong perturbations of the surface, having CO molecules also free access to any cavity and avoiding steric hindrances.<sup>14,15</sup> This is a good opportunity to evaluate “pure acidity” without any steric constraint,<sup>16</sup> and has been applied to both HMOR and NaMOR.<sup>17,18</sup> By contrast, the adsorption of a set of differently hindered nitriles allowed investigation of the accessibility and the multiplicity of the protonic sites on H–mordenite<sup>19,20</sup> and on cobalt-exchanged mordenite.<sup>21</sup>

In this paper we describe the results of an IR study of the adsorption of different hindered nitriles on Na–mordenite. The results will be compared with those of low temperature CO adsorption measurements. The aim is to have indications of the locations and accessibility of the adsorption sites of Na–mordenite.

## Experimental Section

Mordenite has been used as the main object of study of this work. NaMOR (Si/Al = 6.5, CBV 10A, Lot No. 1822-50) was supplied by Zeolyst as hydrated powder. The chemical composition was SiO<sub>2</sub>/Al<sub>2</sub>O<sub>3</sub> mole ratio 13 and 6.6 wt % Na<sub>2</sub>O. HMOR was prepared by cation exchanging the starting form, NaMOR, with a 2.2 M NH<sub>4</sub>Cl solution and later calcining at 673 K for 12 h.

Other materials (NaX and Na–silica–alumina) have also been used to clarify some results obtained with mordenite for comparison. NaX zeolite was supplied by Rhône Poulenc. Na–silica–alumina was prepared by impregnation of a commercial silica–alumina from STREM with a Na<sub>2</sub>CO<sub>3</sub> solution. The impregnation was carried out so that the moles of Na<sup>+</sup> ions introduced was equal to the moles of aluminum atoms in the commercial silica–alumina.

Mordenite samples were characterized using the following techniques: Powder X-ray diffraction patterns of the samples were obtained with a Siemens D5000 diffractometer (Bragg–Brentano parafocusing geometry and vertical  $\theta$ – $\theta$  goniometer) fitted with a curved graphite diffracted-beam monochromator, incident and diffracted-beam Soller slits, a 0.006° receiving slit, and scintillation counter as a detector. The angular  $2\theta$  diffraction range was between 5° and 70°. The data were collected with an angular step of 0.05° at 3 s per step and sample rotation. Cu K $\alpha$  (1.542 Å) radiation was obtained from a copper X-ray tube operated at 40 kV and 30 mA. The cell parameters and cell volume values were calculated using a matching profile with TOPAS 2.0 software (Bruker AXS).

\* To whom correspondence should be addressed. Telephone: +39-10-3536020. Fax: +39-10-3536028. E-mail: Guido.Busca@unige.it.

<sup>†</sup> Università di Genova.

<sup>‡</sup> Universitat Rovira i Virgili.

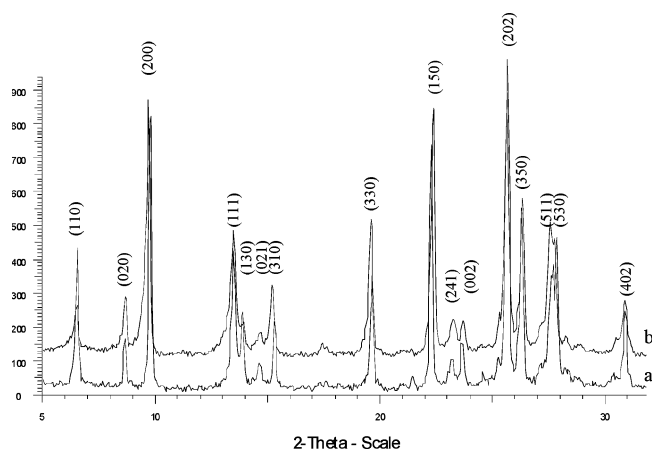


**Figure 1.** X-ray diffraction patterns of NaMOR (a) and HMOR (b) samples.

**TABLE 1: Cell Parameters of HMOR and NaMOR Samples Calculated by XRD**

	<i>a</i> (Å)	<i>b</i> (Å)	<i>c</i> (Å)	cell vol (Å <sup>3</sup> )
HMOR	18.098 (4)	20.447 (3)	7.510 (1)	2279
NaMOR	18.180 (4)	20.315 (3)	7.484 (1)	2764

Skeletal mid-IR (KBr pressed disks) and far-IR (pure powder on polyethylene supports) spectra were recorded on a Nicolet Magna 750 Fourier transform instrument (resolution 4 cm<sup>-1</sup>). Additionally, both samples were characterized (in the mid-IR range) by adsorbing several probe molecules. Different nitriles such as acetonitrile (AN), propionitrile (PrN), isobutyronitrile (IBN), pivalonitrile (PN), benzonitrile (BN), and *o*-toluonitrile (*o*-TN) were used to characterize mordenite samples, and furthermore CO at low temperature was also used. The pressed disks of pure zeolite powders were activated “in situ” the IR cell by outgassing at 773 K before the adsorption experiments. A conventional gas manipulation/outgassing ramp connected to the IR cell was used.

The adsorption/desorption process has been studied by transmission Fourier transform infrared (FT-IR) spectroscopy. For nitriles, the adsorption procedure involves contact of the activated sample disk with vapors at room temperature at a pressure not higher than 2.5 kPa. The desorption process at increasing temperatures was performed in vacuum compressed at temperatures in the range 273–573 K. On the other hand, CO adsorption was performed at 130 K by the introduction of a well-known dose of the gas inside the low temperature infrared cell containing the previously activated wafers. IR spectra were collected on evacuation at increasing temperatures between 130 and 273 K. Additionally, the coadsorption of acetonitrile and CO was performed in a way that first acetonitrile was adsorbed at room temperature and subsequently evacuated at 373 K. Consecutively, the cell temperature was decreased to 130 K and a well-known dose of CO was introduced, which was subsequently evacuated at temperatures between 130 and 273 K.

## Results and Discussion

**1. Skeletal Mid-IR and Far-IR Spectra.** Figure 1 shows the X-ray diffraction patterns obtained for NaMOR and HMOR samples, which agree with the respective mordenite JCPDS files. The calculated cell parameters and cell volume for both samples are also reported in Table 1. Both samples present similar crystallinity, and no significant differences in the peak width and peak intensity are appreciable from X-ray patterns in Figure 1. However, the cell parameter values indicate an increase of

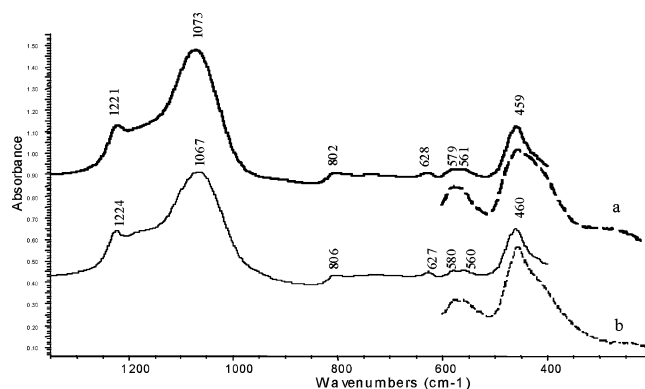


**Figure 2.** Skeletal mid-IR (continuous line) and far-IR (discontinuous line) of HMOR (a) and NaMOR (b) samples.

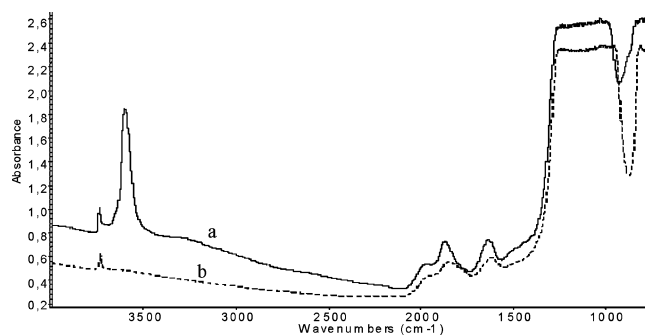


**Figure 3.** FT-IR spectra of activated HMOR (a) and NaMOR (b) samples at 773 K under vacuum conditions.

the cell dimensions from HMOR to NaMOR, which can be assigned to the effect of the different dimensions of H<sup>+</sup> and Na<sup>+</sup> cations in the cavities and to a certain dealumination during HMOR preparation. In both NaMOR and HMOR X-ray patterns only *hkl* peaks assigned to the mordenite framework can be observed. Consequently, the absence of *hkl* peaks associated with a cation matches in structure, suggesting that cations may be randomly distributed on our material, in agreement with an higher disorder found for synthetic versus natural mordenite samples.<sup>22,23</sup>

In Figure 2, the skeletal IR spectra (KBr pressed disks) for HMOR and NaMOR are reported. The spectra compare well with those reported in the literature. The substitution of Na<sup>+</sup> cations for H<sup>+</sup> causes a slight shift to higher frequencies of the main maximum in the massive asymmetric mode probably related to some dealumination in the preparation process.<sup>24</sup> Also, in far-IR spectra no differences associated with the cation type present can be distinguished in both samples. In particular, no bands are observed in the region below 450 cm<sup>-1</sup>, where Na–oxygen stretching modes are expected and found, e.g., in the case of NaX zeolite.<sup>24</sup> This agrees with an at least partially random distribution of Na<sup>+</sup> cations in the structure.

**2. Spectra of the Surface Hydroxy Groups.** The overall spectrum of activated NaMOR sample (pure powder pressed disks) in the 4000–900 cm<sup>-1</sup> range is compared to the spectrum of HMOR sample in Figure 3. In the OH stretching region for HMOR sample, two bands can be observed: the first at 3744 cm<sup>-1</sup> associated with the terminal silanol groups, and the second one (very strong and complex), with the main maximum at 3605 cm<sup>-1</sup>, assigned to the bridging Si–OH–Al groups. According to Bevilacqua et al. such OH groups are exclusively located on the inner surface and possess a strong Brønsted acidity.<sup>19,20</sup> The asymmetry of this band indicates the presence of different components. At least three components were previously identified by Bevilacqua et al.<sup>19,20</sup> and later confirmed by Marie et

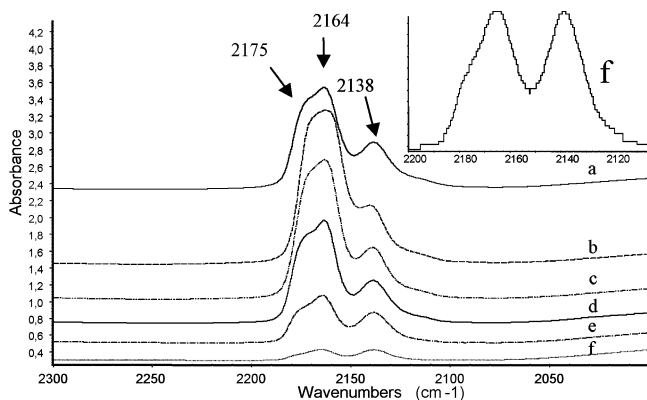


**Figure 4.** FT-IR spectra of NaMOR in the presence of CO gas at 133 K (a), and under evacuation at 143 (b), 173 (c), 193 (d), 213 (e), and 233 K (f) in the CO stretching range.

al.<sup>17</sup> An additional weak component can be observed for HMOR sample at  $3655\text{ cm}^{-1}$ , which can be associated with small amounts of extraframework aluminum species formed during the activation by heating in vacuo. Meanwhile, for NaMOR, only one small peak at  $3745\text{ cm}^{-1}$  was observed. The absence of the band centered at  $3605\text{ cm}^{-1}$  indicates that all possible cationic positions are occupied by  $\text{Na}^+$  cations in the NaMOR sample. In contrast, the band corresponding to terminal silanol groups has roughly the same intensity and position in both samples, suggesting that external silanols are not affected by cation exchange.

In the  $2100\text{--}1500\text{ cm}^{-1}$  region, three typical skeletal overtones are found like those on any silica-based material, while in the region between  $1300$  and  $1000\text{ cm}^{-1}$  a cutoff is observed due to the Si—O—Si(Al) asymmetric stretching skeletal mode. In agreement with the shift observed for the main maximum near  $1070\text{ cm}^{-1}$  in the skeletal spectrum (KBr disks), also in the pure powder pressed disk spectrum, both overtones and fundamental skeletal bands are slightly shifted to lower frequencies for NaMOR with respect to HMOR.

**3. Low Temperature Adsorption of CO on NaMOR and HMOR.** Adsorption of CO at low temperature has been carried out on both zeolites (Figures 4–6). Figure 4 shows the IR bands of adsorbed CO on NaMOR. At 133 K (real adsorption temperature as measured on the sample when liquid nitrogen is in the external cooling jacket) two main bands are observed in the CO stretching range: the first one, more intense, has the main maximum at  $2164\text{ cm}^{-1}$  and a shoulder at  $2175\text{ cm}^{-1}$ , and the second one, less intense, is located at  $2138\text{ cm}^{-1}$ . By progressively increasing temperature upon outgassing, the higher frequency band and its shoulder correspondingly decrease their intensity. In the same way, the lower frequency band decreases on intensity, but much more slowly, when temperature increases. However, this band, which is initially weaker than the higher frequency band, has finally a similar intensity at 213 and 233 K. In the OH vibration range (not shown here), the band at  $3745\text{ cm}^{-1}$  is not perturbed, indicating that terminal silanol groups do not interact with CO molecules under these conditions.

The band at  $2164\text{ cm}^{-1}$  and its shoulder at  $2175\text{ cm}^{-1}$  have been previously identified by other authors. Marie et al. have found them at  $2163$  and  $2174\text{ cm}^{-1}$  for NaMOR (Si/Al ratio 10).<sup>17</sup> Bordiga et al. reported the frequency of those bands at  $2159$  and  $2177\text{ cm}^{-1}$  for NaMOR (Si/Al of 5).<sup>18</sup> In both papers, taking into account the respective polarizing properties of cations depending on the location in the zeolitic structure, the component at lower frequency has been assigned to the C-bonded CO

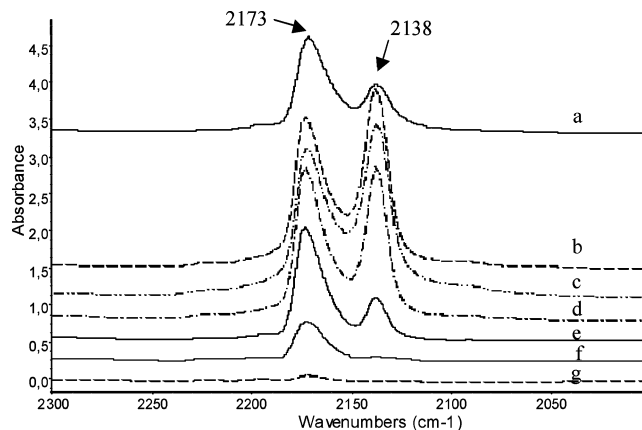


**Figure 5.** FT-IR spectra of HMOR in the presence of CO gas taken immediately at 133 K (a) and after 2 min (b), and under evacuation at 133 (c), 143 (d), 173 (e), 193 (f), and 213 K (g) in the CO stretching range.

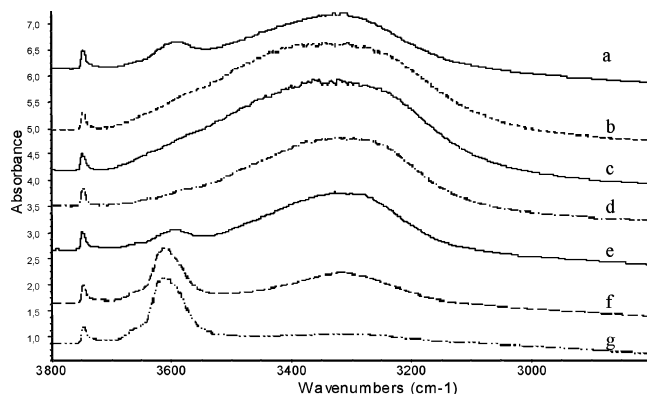
interacting with  $\text{Na}^+$  cations located in the side pockets, while the component at higher frequency has been associated with the CO interacting with those located in the main channels.

The band at  $2138\text{ cm}^{-1}$  (wavenumber value which is very near that of liquid CO) can be attributed to pseudoliquid physisorbed CO inside the zeolite pores with hindered rotation,<sup>15,17,18</sup> which should desorb or evaporate quite quickly. However, from our spectra, the intensity of this band decreases more slowly than expected for pseudoliquid physisorbed CO, even more slowly than those two higher frequency bands. Therefore, this disagrees with the assignment of this band to liquidlike CO only. In our opinion two superimposed bands are present. The initial decrease of the band could be due to an evaporation of pseudoliquid CO, which should be responsible for only part of this band, but the subsequent so slow decrease in the intensity is evidence of the existence of an additional stronger interaction involving  $\text{Na}^+$  cations. This interaction cannot be apparently attributed to O-bonded CO species ( $\text{Na}^+\cdots\text{OC}$ ), since this interaction has been reported to absorb at lower frequencies (between  $2220$  and  $2212\text{ cm}^{-1}$ ).<sup>15,25</sup> The possibility of the formation of CO species interacting with two  $\text{Na}^+$  ions will be discussed below.

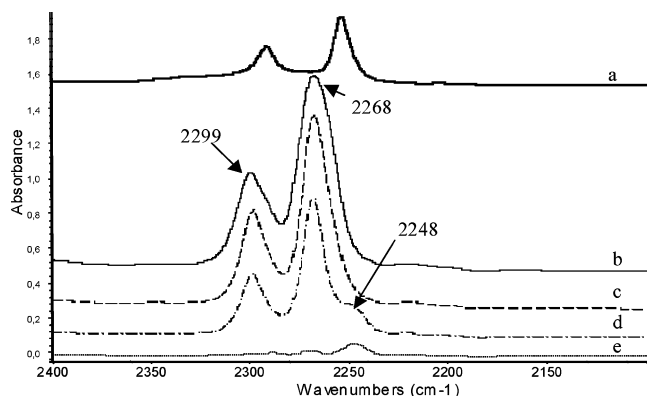
The adsorption of CO on HMOR gives rise, in the CO stretching range, again to two bands: one, the first formed and last disappeared during outgassing, centered at  $2173\text{ cm}^{-1}$  with a tail toward lower frequencies; and the other one, again at  $2138\text{ cm}^{-1}$  (Figure 5). In that case, contrary to what was observed for NaMOR, we are unable to single out two components for the CO stretching band of C-bonded CO interacting with  $\text{H}^+$  located in the main channels and side pockets. In that case, the band at  $2138\text{ cm}^{-1}$  disappears progressively upon outgassing and can consequently be assigned, with confidence, to the pseudoliquid CO. This further supports the idea that part of the band at  $2138\text{ cm}^{-1}$  on NaMOR is something associated with interactions of CO molecules with  $\text{Na}^+$  cations.

Figure 6 shows the effects of the CO adsorption on HMOR in the OH vibration range. The band at  $3745\text{ cm}^{-1}$  is not perturbed as for the NaMOR sample. Otherwise, just after contacting the surface with CO (Figure 6a), only part of the bridging OH band at  $3605\text{ cm}^{-1}$  shifts to near  $3300\text{ cm}^{-1}$ , and a residual band is still present at  $3590\text{ cm}^{-1}$ . After more prolonged contact, this component at  $3590\text{ cm}^{-1}$  disappears and the band of the OH, interacting with CO, seems to present an additional component at higher frequencies (around  $3400\text{ cm}^{-1}$ ). By evacuating, the situation seems to be exactly reversed, since,





**Figure 6.** FT-IR spectra of HMOR in the presence of CO gas taken immediately at 133 K (a) and after 2 min (b), and under evacuation at 133 (c), 143 (d), 173 (e), 193 (f), and 213 K (g) in the OH vibration range.



**Figure 7.** FT-IR spectra of AN in CCl<sub>4</sub> solution (a), NaMOR in the presence of AN vapors (b), and AN after evacuation at room temperature (c), 373 K (d), and 473 K (e).

in the first place, the component near 3590 cm<sup>-1</sup> is restored, when the absorption near 3400 cm<sup>-1</sup> disappears, while the band at 3605 cm<sup>-1</sup> is restored later. Our conclusion is that CO adsorbs first on OHs in the main channels and later, more slowly, diffuses into the side pockets. The OHs located in the side pockets, responsible for the 3590 cm<sup>-1</sup> band, are less perturbed than those in the main channels upon interaction with CO. This may be due to a higher acidity of OHs in the main channels or to some hindering of the interaction occurring in the side pockets in agreement with Hadjiivanov et al.<sup>15</sup> and Maache et al.<sup>26</sup>

**4. IR Study of the Adsorption of Acetonitrile and Propionitrile.** Acetonitrile (AN) adsorption has been used for characterizing the different hydroxy groups of H-zeolites including HMOR, since they can access all protonic sites on HMOR.<sup>19,27</sup> AN adsorption has also been investigated on NaY and NaX.<sup>28,29</sup>

The spectra of AN adsorbed on NaMOR sample, and after outgassing at different temperatures, are shown in Figure 7. The activated sample spectrum as well as the gas-phase spectrum has been subtracted from all spectra. The same procedure has been applied to all adsorption experiments reported in this work. The nitrile spectrum on CCl<sub>4</sub> solution, used as a reference, is also shown.

From the subtracted spectra obtained in contact with AN vapor and evacuated at room temperature (Figure 7b,c) two bands at 2268 and 2299 cm<sup>-1</sup> can be observed in the CN stretching region. It is well-known that the AN CN stretching mode gives place to two bands due to the Fermi resonance between the fundamental stretching CN with a  $\delta_{\text{CH}_3} + \nu_{\text{C}-\text{C}}$  combination. Both bands are slightly asymmetric with a tail

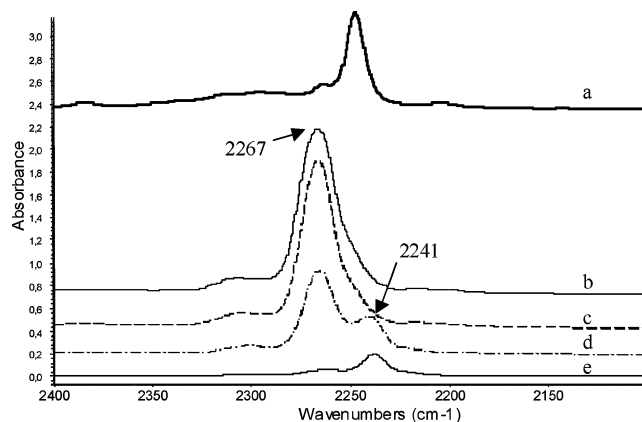


**Figure 8.** FT-IR spectra of PrN in CCl<sub>4</sub> solution (a), NaMOR in the presence of PrN vapors (b), and PrN after evacuation at room temperature (c), 373 K (d), and 473 K (e).

toward lower frequencies. By evacuating, the bands become narrower since the tail at lower frequencies seems to disappear. In the desorption process, by increasing the temperature under vacuum, the intensity of these bands in the CN region decreases; additionally, when outgassing at 373 and 473 K (Figure 7d,e) a new band at 2248 cm<sup>-1</sup> is also observed, possibly with a further Fermi resonance component near 2270 cm<sup>-1</sup>. The position of the main CN Fermi resonance bands (2268 and 2299 cm<sup>-1</sup>) of adsorbed AN is, as usual, shifted to higher frequencies than those observed in CCl<sub>4</sub> diluted solution. In contrast, the doublet still present after outgassing at 473 K is observed at slightly lower frequencies than in CCl<sub>4</sub> solution.

The subtracted spectra of PrN adsorbed on NaMOR sample and after outgassing at different temperatures are shown in Figure 8. For propionitrile adsorption on NaMOR, one asymmetric band with a maximum at 2267 cm<sup>-1</sup> can be observed on the CN stretching in the presence of PrN vapors. The tail observed toward lower frequencies starts to disappear upon evacuation at room temperature (Figure 8b,c). With increasing temperature, the band intensity decreases and a new component at 2241 cm<sup>-1</sup> appears at 373 K (Figure 8d,e). Again the main band is definitely at a higher frequency than that observed for the nitrile in CCl<sub>4</sub> solution, whereas the band appearing after evacuation at 473 K is at lower frequencies.

The main bands at 2299 and 2268 cm<sup>-1</sup> observed for AN adsorbed on NaMOR can be assigned to the same interaction of CN group with Na<sup>+</sup> cations observed for AN adsorbed on NaY (2293 and 2263 cm<sup>-1</sup>)<sup>28</sup> and on NaX (2296 and 2267 cm<sup>-1</sup>),<sup>29</sup> and also for the Na(CH<sub>3</sub>CN)<sub>3</sub><sup>+</sup> complex in solution (2302 and 2270 cm<sup>-1</sup>).<sup>30</sup> Moreover, the lower frequency tails observed could be attributed to the CN group interaction with terminal silanol groups since in the OH region (not shown here) it is clear that the terminal silanol groups are perturbed on contact with nitrile vapors, since the OH band at 3745 cm<sup>-1</sup> disappears and a broad new band centered around 3450 cm<sup>-1</sup> is observed. The easy recovery of the silanol band by outgassing at room temperature together with the CN stretching tail disappearance indicates the weakness of that interaction.

A parallel situation is found for PrN. The main band at 2267 cm<sup>-1</sup>, shifted well above the band in CCl<sub>4</sub> solution, is assigned to the interaction with Na<sup>+</sup>, while the tail at lower frequencies is assigned to the interaction with external silanols.

The nature of the species responsible for the bands at 2270 and 2248 cm<sup>-1</sup> for AN and at 2241 cm<sup>-1</sup> for PrN adsorption experiment is not straightforward. To our knowledge, there is no case in the literature in which an interaction between nitriles

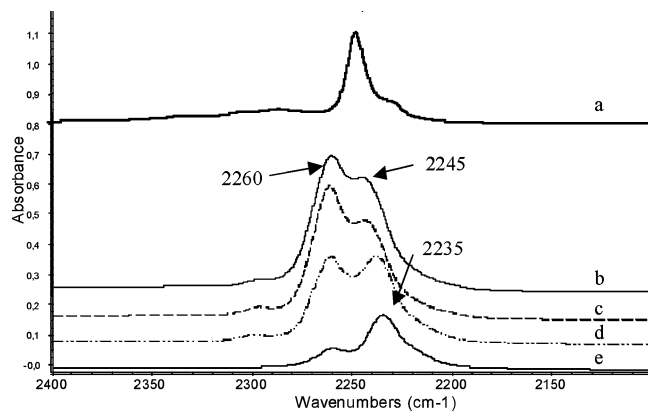


**Figure 9.** FT-IR spectra of IBN in  $\text{CCl}_4$  solution (a), NaMOR in the presence of IBN vapor (b), and IBN after evacuation at room temperature (c), 373 K (d), and 473 K (e).

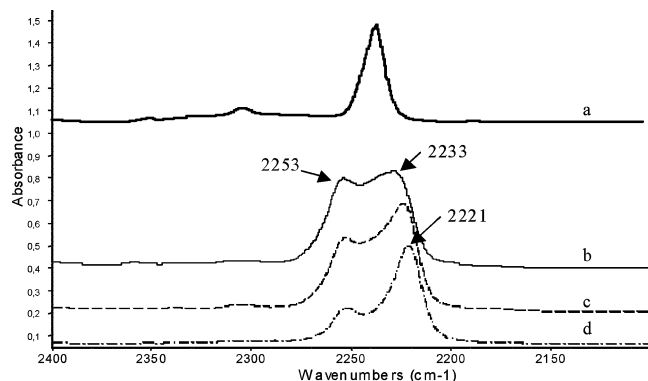


**Figure 10.** FT-IR spectra of PN in  $\text{CCl}_4$  solution (a) and on NaMOR after evacuation at room temperature (b), 373 K (c), and 473 K (d).

and zeolitic sites gives rise to an IR absorption band at lower frequencies than the corresponding band observed for the liquid (Figures 7a and 8a).

Interestingly, this seems to parallel what happens with CO on NaMOR, which also gives rise to a quite strongly adsorbed species characterized by absorbing at slightly lower frequencies than that observed for free CO.

To try to clarify this phenomenon, we studied the adsorption of more hindered nitrile probe molecules.

**5. IR Study of the Adsorption of Isobutyronitrile and Pivalonitrile.** Isobutyronitrile (IBN) and pivalonitrile (PN) have been previously used for the characterization of different hydroxy groups in HMOR samples.<sup>19,20</sup> It has been shown that because of the higher steric hindrance of the nitrile alkyl group they do not access all the OH groups on HMOR; in particular, IBN does not seem to access the side pockets and PN only interacts with OHs pointing to the center of the main channels.

The subtracted adsorption/desorption spectra obtained for NaMOR samples using isobutyronitrile (IBN) and pivalonitrile (PN) vapors as probe molecules are shown in Figures 9 and 10, respectively. The spectra of IBN on NaMOR after adsorption and evacuation at increasing temperatures are shown in Figure 9b–e. In all cases at least two bands with maxima at 2260 and 2245  $\text{cm}^{-1}$  are observed. Intensity diminishes by increasing outgassing temperature, but interestingly, the band at lower frequencies does it more slowly. While the position of the band at higher frequencies remains invariable, the band at lower frequencies further shifts to lower frequencies (until 2235  $\text{cm}^{-1}$ ) when the outgassing temperature increases. Again, this component is at lower frequencies than that in  $\text{CCl}_4$  solution, while the other component is at higher frequencies.

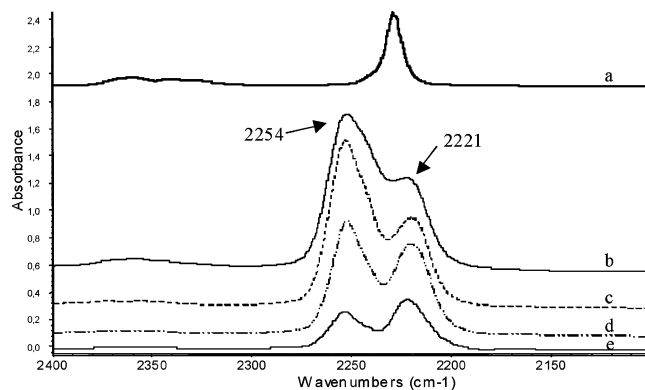


**Figure 11.** FT-IR spectra of liquid BN (a), NaMOR in the presence of BN vapor (b), and BN after evacuation at room temperature (c), 373 K (d), and 473 K (e).

Adsorption/desorption behavior observed for PN on NaMOR is similar to that observed for IBN. The spectrum of the CN stretching region obtained at room temperature in the presence of PN vapors shows two bands with maxima at 2253 and 2233  $\text{cm}^{-1}$  (Figure 10b). Again, when temperature increases, the bands resolution improves and a decrease in the intensity is also observed. During the desorption process at increasing temperatures (Figure 10c,d), as reported above for IBN, a shift is observed for the lower frequency band, down to 2221  $\text{cm}^{-1}$  at 373 K. Also, in that case, that band at lower frequencies shows a higher resistance to the desorption process, since its intensity at 373 K is much higher than that found for the previously used probe molecules.

In both cases, when NaMOR contacts with nitrile vapors, the band corresponding to the terminal silanol groups (at 3745  $\text{cm}^{-1}$ ) disappears and the previously noted band at 3450  $\text{cm}^{-1}$  is formed. As previously noted, the silanol–nitrile interaction is weak, since the corresponding OH band is restored by evacuating at room temperature.

Interestingly, the highest intensity ratio between the lower and higher frequency bands was obtained for PN among all the nitriles tested so far. Therefore, in the case of PN, whose access to the channels is highly hindered, the CN stretching band shifted to lower frequencies and the liquid appears to be much stronger than in the case of nitriles with less restricted access to the channels such as AN, PrN, and IBN.

Due to the fact that the more hindered nitriles give rise to a stronger interaction, additional adsorption studies with other kinds of hindered nitriles, such as aromatic nitriles, have been performed.

**6. IR Study of the Adsorption of Benzonitrile and *o*-Toluenitrile.** Subtracted spectra of benzonitrile (BN) and *o*-toluenitrile (*o*-TN) adsorbed on NaMOR and after evacuation at increasing temperatures are shown in Figures 11 and 12, respectively. The spectra of the nitrile molecules on NaMOR show in the CN stretching region two peaks, whose main maxima are centered at 2254 and 2221  $\text{cm}^{-1}$  for BN and at 2246 and 2216  $\text{cm}^{-1}$  for *o*-TN. In both cases, at room temperature, the intensity of the bands at higher frequency is higher than those at lower frequency, but during the desorption process, the intensity of the first ones decreases faster, until they have a similar intensity. Comparing those frequencies with that of the nitrile spectra in  $\text{CCl}_4$  solution (Figure 11a for BN and Figure 12a for *o*-TN), we observe again that one band is located at higher and the other band at lower frequencies. However, in these samples the intensity ratio between the lower and the higher frequency bands is lower than for PN and IBN,

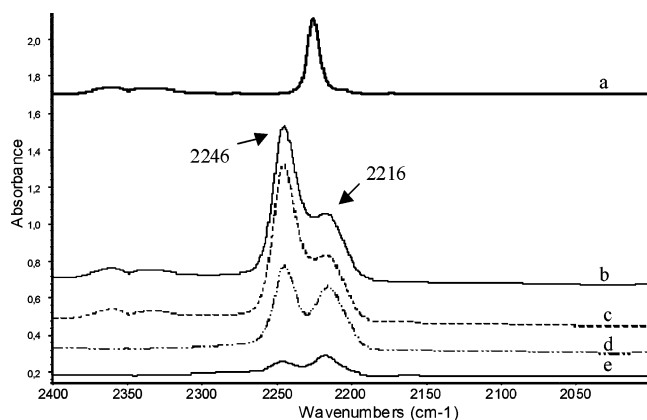


**Figure 12.** FT-IR spectra of liquid *o*-TN (a), NaMOR in the presence of *o*-TN (b), and *o*-TN after evacuation at room temperature (c), 473 K (d), and 573 K (e).

**TABLE 2: Peak Area Relation for Aliphatic Nitriles with Respect to AN, in CCl<sub>4</sub> Solution (*L*) and Adsorbed on NaMOR (*A*)**

	<i>L</i>	<i>A</i>	<i>A/L</i>
AN	1	1	1
PrN	1.14	0.90	0.79
IBN	1.65	0.45	0.27
PN	1.56	0.32	0.20

but higher than for AN and PrN. Thus, although the hindering influence has been corroborated, additional factors should be involved.

Therefore, for all nitriles tested, a new band due to species more resistant to outgassing, whose CN stretching frequency is shifted to lower frequencies, is formed. This band is more intense for the more hindered nitriles (that do not access the cavities) than for smaller molecules. This indicates that the interaction takes place on the outer surface or on the mouth of the main channels. The interpretation that we can propose for these species is to hypothesize a complex and probably multiple interaction of CN groups with Na<sup>+</sup> cations or Na<sup>+</sup> cations and framework oxygens.

Besides, the CN stretching band shifted downward is more resistant to outgassing than the band shifted upward for nitriles whose access even to the main channels is very highly hindered (PN, BN, and *o*-TN), whereas for the smaller molecules (AN, PrN, and IBN) this band is relatively weaker. To explain the adsorption behavior obtained for these nitriles, a comparative discussion is presented, for which aromatic nitriles have not been taken into account since the comparison becomes difficult due to their different nature. Table 2 shows the relation between peak areas obtained for aliphatic nitriles with respect to the acetonitrile one. Liquid phase nitrile spectra have been collected in diluted CCl<sub>4</sub> solution using quantitative conditions. Peak areas obtained for adsorbed nitrile spectra have been normalized to the disk weight. The data show that the absolute intensity of the CN stretching modes (in the case of AN both components of the Fermi resonance doublet have been considered) tends to increase in the order AN < PrN < IBN ≈ PN in CCl<sub>4</sub> solution (Table 2), while exactly the inverse tendency is found for nitriles adsorbed on NaMOR, where the amount of nitrile adsorbed follows the trend AN > PrN ≫ IBN > PN. This can be easily understood considering that AN and PrN have free access to the main channels and side pockets, while for IBN and PN access to the side pockets is likely forbidden. Taking into account the dimensions of the main channels (6.7 Å × 7.0 Å) and the ionic radius of the Na<sup>+</sup> cations (0.95 Å), as well as the critical diameter of the isopropyl group (5 Å) and *tert*-butyl

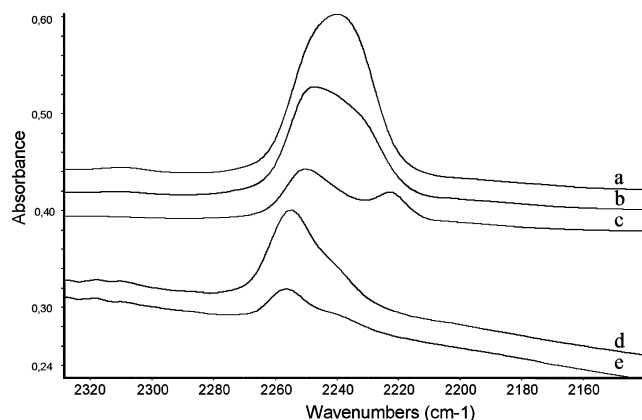


**Figure 13.** FT-IR of adsorbed PN on NaX evacuated at room temperature (a), at 373 (b) and 473 K (c), and on Na-silica-alumina evacuated at room temperature (d) and 373 K (e).

group (6 Å), i.e., alkyl groups of IBN and PN, respectively, it is easy to conclude that the access of PN to the main channels is likely forbidden, but even that for IBN is probably highly hindered. Therefore, the spectrum observed for adsorbed AN is essentially the result of the sum of the spectra of AN in the side pockets, in the main channels, and in the outer surface. In contrast, the spectra of adsorbed PN are only due to the interaction occurring on the outer surface and on the channel mouths. The cases of PrN and IBN are somehow intermediate.

The adsorption of a hindered nitrile, PN, has been investigated also on a commercial Na-X zeolite and on a silica-alumina highly impregnated with Na<sup>+</sup> cations for comparison. The spectra of PN adsorbed on NaX zeolite are reported in Figure 13a-c, where the CN stretching band of adsorbed PN is found, quite broad, after outgassing at room temperature at 2240 cm<sup>-1</sup>. By outgassing at progressively higher temperatures, the intensity band decreases and the main maximum shifts to higher frequency up to 2250 cm<sup>-1</sup>, showing some heterogeneity of the adsorption sites. The maximum rises to a position (but shifted a little downward) similar to that found for NaMOR. However, also in this case upon outgassing at 473 K a component appears at lower frequency, namely at 2223 cm<sup>-1</sup>, near the same position as observed for NaMOR under the same conditions.

In the case of PN adsorption on Na-silica-alumina (Figure 13d,e), the main band is again observed well shifted upward, at even higher frequencies (2257 cm<sup>-1</sup>), with a shoulder centered near 2238 cm<sup>-1</sup>, but in this case, the lower frequency component does not appear. This supports the idea that the complex interaction responsible for the lower frequency band occurs at the mouths of the channels.

**7. Coadsorption AN + CO.** The coadsorption of AN and CO has been performed as described in the Experimental Section. The obtained spectra are shown in Figure 14.

As we have previously described, the maxima of the bands of adsorbed AN on NaMOR slightly shift to higher frequencies upon outgassing at increasing temperatures. This shows the heterogeneity of the adsorption sites. After outgassing at 373 K the intensity of the band diminishes a factor of 0.3. This indicates that AN is desorbed from the weaker sites, while still interacting with the stronger ones, and by coadsorbing CO under these conditions the spectra now show two bands at 2164 and 2138 cm<sup>-1</sup>. The shoulder at higher frequencies (2175 cm<sup>-1</sup>), which is present when adsorbing only CO (Figure 4), is absent here. Therefore, CO is able to access the weakest sites, which have been freed by AN, while it cannot displace the AN adsorbed on the stronger sites. However, interestingly, the low



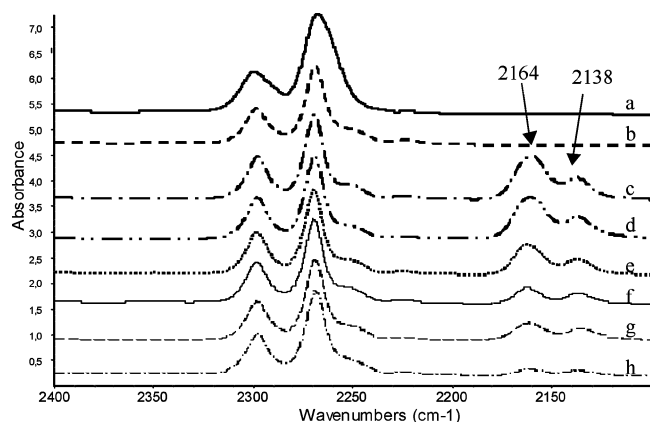


**Figure 14.** FT-IR of adsorbed AN on NaMOR at room temperature (a) evacuated at 373 K and cooled at 133 K (b) after CO adsorption at 133 K (c), and under evacuation at 143 (d), 173 (e), 193 (f), 213 (g), and 233 K (h).

frequency component at 2138  $\text{cm}^{-1}$  is already formed just after contact with CO.

## Conclusions

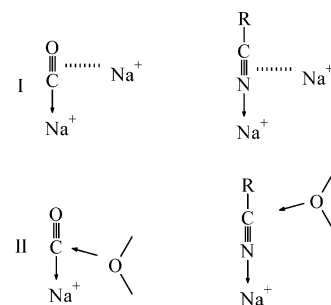
The data described and discussed above may allow us to have deeper information on the NaMOR structure, where X-ray diffraction patterns and skeletal far-IR spectra suggest that  $\text{Na}^+$  cations are randomly matched on the mordenite cavities, and on its interaction with several adsorbates.

Low temperature CO adsorption experiments show two different  $\text{Na}^+\cdots\text{CO}$  complexes characterized by different frequencies that are enhanced with respect to the free molecule spectrum. These complexes can be assigned to single CO molecules interacting with single  $\text{Na}^+$  cations in two different positions—main channels and side pockets. Parallel experiments performed on HMOR show quite clearly that CO first interacts with the Brønsted sites located on the main channels and later diffuses into those located in the side pockets. By outgassing, CO molecules first desorb from the sites located in the side pockets and later leave those of the main channels. This behavior agrees with the stronger perturbation of the OHs located in the main channels showing, in agreement with Maache et al.,<sup>24</sup> that the OHs in the main channels are likely more acidic, or in any case give a stronger interaction with CO, than those in the side pockets. Thus, in HMOR interaction with so small a molecule as CO, adsorption/desorption phenomena are mostly determined by adsorption strength rather than by diffusion phenomena.

However, in the case of CO adsorption on NaMOR, a third, even stronger and perhaps activated, adsorption mode seems to occur. According to our results, the band observed at 2138  $\text{cm}^{-1}$ , and previously assigned to liquidlike CO, contains an additional component that resists outgassing at 233 K. This quite stable species should be assigned to CO molecules involved in a multiple interaction that causes a slight decrease in the CO stretching frequency. Because these species not observed on HMOR, it seems likely that this interaction involves  $\text{Na}^+$  cations.

Adsorption of nitriles characterized by differently hindered hydrocarbon entities shows in all cases the formation of complexes with  $\text{Na}^+$  cations. The adsorption of AN shows a clear heterogeneity of the adsorption sites and shows that, as expected, the species characterized by the stronger perturbation are more resistant when outgassing. Also, in this case, consequently, adsorption/desorption phenomena seem to be mostly determined by adsorption strength rather than by diffusion phenomena. In the case of PN, which was previously found to

## SCHEME 1: Tentative Structures for the Strongest Interactions of CO and Nitriles on NaMOR<sup>a</sup>



<sup>a</sup> I, interactions with two  $\text{Na}^+$  ions; II, interaction with  $\text{Na}^+$  and  $\text{O}^{2-}$  ions.

access, very slowly, only the main channels of HMOR, access to the cavities of NaMOR is likely fully forbidden. This is also very likely the case of BN and *o*-TN. However, although such big hydrocarbon entities cannot enter the cavities, CN can do this by interacting with the  $\text{Na}^+$  cations located either at the external surface or near the mouth of the main channels.

For all nitriles, in addition to that band with a CN stretching frequency located at higher frequencies than the liquid value (CN shift 15–20  $\text{cm}^{-1}$ ), a new band is formed at frequencies near or slightly below the liquid value, whose stability seems to be higher than the usual ones. The behavior observed for all nitriles, at 300–500 K seems to parallel that observed for CO at 150–250 K. A new band associated with more resistant species is observed, with a CN stretching frequency shifted lower than the liquid value. The interpretation that we propose for these species is to hypothesize multiple interactions where CN groups interact with  $\text{Na}^+$  cations or  $\text{Na}^+$  cations and framework oxygen atoms (see Scheme 1 for possible structures). The fact that this interaction is more important for highly hindered molecules together with the fact that it does not appear on Na-silica-alumina, where zeolitic pores do not exist, suggests that the interaction takes place on the mouth of the main channels.

**Acknowledgment.** The authors are grateful to the Generalitat de Catalunya (2002FI 00667).

## References and Notes

- (1) *Zeolites for cleaner technologies*; Guisnet, M.; Gilson, J. P., Eds.; Imperial College Press: London, 2002.
- (2) van Bokhoven, J. A.; Tromp, M.; Koningsberger, D. C.; Miller, J. T.; Pieterse, J. A. Z.; Lercher, J. A.; Williams, B. A.; Kung, H. H. *J. Catal.* **2001**, 202, 129.
- (3) Moreau, F.; Ayrault, P.; Gnep, N. S.; Lacombe, S.; Merlen, E.; Guisnet, M. *Microporous Mesoporous Mater.* **2002**, 51, 211.
- (4) Weitkamp, J.; Hunger, M.; Rymas, U. *Microporous Mesoporous Mater.* **2001**, 48, 255.
- (5) Davis, R. J. *J. Catal.* **2003**, 216, 396.
- (6) Martra, G.; Ocule, R.; Marchese, L.; Centi, G.; Coluccia, S. *Catal. Today* **2002**, 73, 83.
- (7) Armaroli, T.; Finocchio, E.; Busca, G.; Rossini, S. *Vib. Spectrosc.* **1999**, 20, 85.
- (8) Pamba, M.; Maurin, G.; Devautour, S.; Vanderschueren, J.; Giuntini, J. C.; Di Renzo, F.; Hamidi, F. *Phys. Chem. Chem. Phys.* **2000**, 113, 4498.
- (9) Devautour, S.; Abdoulaye, A.; Giuntini, J. C.; Henn, F. *J. Phys. Chem. B* **2001**, 105, 9297.
- (10) Bell, R. G.; Devautour, S.; Henn, F.; Giuntini, J. C. *J. Phys. Chem. B* **2004**, 108, 3739.
- (11) Webster, C. E.; Cottone, A.; Drago, R. S. *J. Am. Chem. Soc.* **1999**, 121, 12127.
- (12) Yuvaray, S.; Chang, T. H.; Yeh, C. T. *J. Phys. Chem. B* **2003**, 107, 4971.
- (13) Salla, I.; Salagre, P.; Cesteros, Y.; Medina, F.; Sueiras, J. E. *J. Phys. Chem. B* **2004**, 108, 5359.

- (14) Knözinger, H.; Huber, S. *J. Chem. Soc., Faraday Trans.* **1998**, 94 (15), 2047.
- (15) Hadjiivanov, K. I.; Vayssilov, G. N. Characterization of oxide surfaces and zeolites by Carbon Monoxide as an IR Probe Molecule. In *Advances in Catalysis*; Academic Press: New York, 2002; Vol. 47, p 307.
- (16) Onida, B.; Monelli, B.; Borello, L.; Fiorilli, S.; Geobaldo, F.; Garrone, E. *J. Phys. Chem. B* **2002**, 106, 10518.
- (17) Marie, O.; Massiani, P.; Thibault-Starzyk, F. *J. Phys. Chem. B* **2004**, 108, 5073.
- (18) Bordiga, S.; Lamberti, C.; Geobaldo, F.; Zecchina, A.; Turnes Palomino, G.; Otero Areán, C. *Langmuir* **1995**, 11, 527.
- (19) Bevilacqua, M.; Gutiérrez-Alejandre, A.; Resini, C.; Casagrande, M.; Ramírez, J.; Busca, G. *Phys. Chem. Chem. Phys.* **2002**, 4, 4575.
- (20) Bevilacqua, M.; Busca, G. *Catal. Commun.* **2002**, 3, 497.
- (21) Montanari, T.; Bevilacqua, M.; Resini, C.; Busca, G. *J. Phys. Chem. B* **2004**, 108, 2120.
- (22) Shiokawa, K.; Ito, M.; Itabashi, K. *Zeolites* **1989**, 9, 170.
- (23) Simoncic, P.; Armbruster, T. *Am. Mineral.* **2004**, 89, 421.
- (24) Busca, G.; Resini, C. Vibrational spectroscopy for the analysis of geological and inorganic materials. In *Encyclopedia of Analytical Chemistry*; Meyers, R. A., Ed.; Wiley: Chichester, 2000; pp 10984–11020.
- (25) Tsyganenko, A. A.; Escalona Platero, E.; Otero Areán, C.; Garrone, E.; Zecchina, A. *Catal. Lett.* **1999**, 61, 187.
- (26) Maache, M.; Janin, A.; Lavalley, J. C.; Benazzi, E. *Zeolites* **1995**, 15, 507.
- (27) Zecchina, A.; Geobaldo, F.; Spoto, G.; Bordiga, S.; Ricchiardi, G.; Buzzoni, R.; Petrini, G. *J. Phys. Chem.* **1996**, 100, 16584.
- (28) Angell, C. L.; Howell, M. V. *J. Phys. Chem.* **1969**, 73, 2551.
- (29) Armaroli, T.; Finocchio, E.; Busca, G.; Rossini, S. *Vib. Spectrosc.* **1999**, 20, 85–94.
- (30) Reedijk, J.; Zuur, A. P.; Groeneveld, W. L. *Recueil* **1967**, 86, 1127.